diffusion-fundamentals.org

The Open-Access Journal for the Basic Principles of Diffusion Theory, Experiment and Application

Water Diffusion in *q*-space Imaging as a Probe of Cell Local Viscosity and Anomalous Diffusion in Grey and White Matter

R.Nicolas[1,2], *F. Aubry*[1,2], *J. Pariente*[1,2], *X. Franceries*[1,2,3], *N. Chauveau*[1,2], *L. Saint-Aubert*[1,2], *F. Chollet*[1,2], *S. Breil*[4] *and P. Celsis*[1,2]

[1] Inserm, Imagerie cérébrale et handicaps neurologiques, UMR 825, F-31059 Toulouse, France
[2] Université de Toulouse, UPS, Imagerie cérébrale et handicaps neurologiques, UMR 825, F-31059 Toulouse, France
[3]Université de Toulouse; UPS, INPT; LAPLACE (Laboratoire Plasma et Conversion d'Energie); F-31062 Toulouse, France
[4]Philips Medical Systems, France

Corresponding author : Renaud NICOLAS, Inserm, Imagerie cérébrale et handicaps neurologiques, UMR 825, F-31059 Toulouse, France. e-mail: rnd.nicolas@gmail.com

(received 13 September 2010, accepted 19 November 2010)

Abstract

Extraction of accurate quantitative parameters to characterize water diffusion in complex porous media like brain tissue in neuroimaging is a challenging inverse problem, that depends on medium's structural and geometrical factors [1,3]. If the role of membranes is generally invoked, probe collisions with the insoluble cytoskeleton network and water hydrodynamic interactions with dissolved macromolecules and cytoskeleton occur as well [2]. The latter two interactions have been shown to determine the phenomenological "anomalous diffusion" of probes in the cytoplasm [4,5,6,7,8]. Additionally, the diffusion of small solutes in cytoplasm could be slowed by the local micro-viscosity of the aqueous phase, a phenomenon generally not taken into account in simulations. We suggest that the Grey and White Matter contrast in Diffusion Decay Imaging (DDI) could be caused by differences in cytoskeleton structures, composed respectively of actin and tubulin that could act by the elimination of one possible water diffusion pathlength by the volume occupied by the network phase. This could explain why anomalous DDI signal has been shown to be independent of membrane integrity [9]. Cytoplasm is able to rapidly shift from a sol (aqueous solutions embedded with insolubles particles) to a gel state (a colloidal solutions with a structured semi-solid and an aqueous fluid phase) or to a viscous solution when the insoluble particles become soluble. Does water have the ability of being a sensor of its local "self-viscosity" ? What is the length of the water diffusion's path compared to cells size ? Compared to this path length, how many cellular structures should be probed by water's translational diffusion ? We try to respond to these questions by investigating Diffusion Decay Imaging models and their effects on the hypothese-free *q*-space diffusion propagator shape [3], containing all informations concerning viscosity-slowed gaussian diffusion, structural informations [3] and restricted diffusion [1].

Keywords : *q*-space, Diffusion Decay Imaging, Cytoplasm, Anomalous Diffusion, Microtubules

Abbreviations : ADI (Anomalous Diffusion Imaging), ADC (Apparent Diffusion Coefficient), ADCk (Kurtosis Apparent Diffusion Coefficient), ADK (Apparent Diffusional Kurtosis), ATP (Adenosine Triphosphate), BEDI (Bi-exponential Diffusion Imaging), CSF (CerebroSpinal Fluid), DDC (Distributed Diffusion Coefficient), DDI (Diffusion Decay Imaging), DKI (Diffusional Kurtosis Imaging), DWI (Diffusion Weighted Imaging), EPI (Echo Planar Imaging), FT (Fourier Transform), FWHM (Full Width at Half Maximum), GM (Grey Matter), GTP (Guanosine Triphosphate), ILT (Inverse Laplace Transform), MEDI (mono-exponential Diffusion Imaging), P(RMSD=0) (Probability of zero-displacement), qSI (q-space Imaging), RAM (Random Acess Memory), RMSD (Root mean Squared Displacement), ROI (Region of Interest), WM (White Matter).

1. Introduction : calculation of Stokes-Einstein law for free and cell water :

First, we verify that Stokes-Einstein law $D_{H_20}=\frac{k_B T}{6\pi\ R_S\ \eta_{H_20}}$ could be valid for free water itself (with H-O radius R_s=0.990 10^{-10} m
and the experimental free water dynamic viscosity η (Pa.s) : $\eta_{H_20}^{37\ °C}=0.7606\ \ 10^{-3}\ \ kg.s^{-1}.m^{-1}$ [10]), by calculating the theoretical diffusion coefficient (SI units) : D_{theo}=3.016 10^{-9} m²/s = 3.016 µm²/ms that we can compare to the experimental measure : D_{exp}=3.05 µm²/ms [11].
Considering the viscosity of cytoplasm as 3-4 fold that of the free water [12], the same calculation leads to a theoretical cytoplasmic diffusion coefficient of 0.754 µm²/ms $< D_{cyto} <$ 1.00564 µm²/ms.
We can then calculate theoretical *RMSDs* (the real quantitative values measured by diffusion NMR) of water in tissue, if the decrease of the diffusion coefficient in brain would be *entirely* due to viscosity and would follow Einstein law : $RMSD=\sqrt{(<r^2>)}=\sqrt{(2n.D.t_d)}$ and with t_d =27.133 ms we obtain a 3D displacement of 11.079 µm < *RMSD*(cell water) < 12.795 µm compared to *RMSD*(free water)=22.28 µm. In anomalous subdiffusion (α<1), the relation observed is : $<r^2(t)>=2n.\Gamma.t_d^{\alpha}$, where α, the anomalous exponent depends on the characteristic fractal walk dimension d_w of the tissue medium ($\alpha=2/d_w$) [13]**.** A low α is associated with a more heterogeneous medium, with a higher number of components of different sizes (increase of medium's fractal dimension). Obstruction of free diffusion at different length scales (cell size, organelles size, tubulin and actin network size, hydrated proteins interaction size …) would cause the anomalous behavior to appear by restriction of water displacement in large scale orders, by barriers of different sizes.

2. Material and Methods

DWI images of a patient were recorded 4 day after stroke in a cortical/subcortical area (Philips 3T Achieva DWI-EPI, *TR/TE*=3179.5/70.5 ms, *b*-factors=0,200,500,1000,2500 s/mm², Δ=34.8 ms, δ=23 ms, t_d=27.133 ms) and registered. We calculated from segmented ROI an averaged S/S_0 signal fitted by ADI model : $S/S_0=\exp[(-b.DDC)^{\alpha}]$ [5,13,14], DKI : $S/S_0=\exp[-b.ADCk+(b^2.ADCk^2.ADK)/6]$ [15], BEDI : $S/S_0=F_{fast.}.\exp(-b.ADC_{fast})+F_{slow.}.\exp(-b.ADC_{slow.})$ or inverted to give *q*-space diffusion propagator ($b=q^2.t_d$) :

$$\bar{p}_s((\boldsymbol{r}-\boldsymbol{r_0}),t_d)=\int_{-\infty}^{+\infty} S(\boldsymbol{q},\boldsymbol{r}-\boldsymbol{r_0},t_d)/S_0\ \ \exp(-i2\pi\,\boldsymbol{q}(\boldsymbol{r}-\boldsymbol{r_0}))\,d^3\boldsymbol{q}$$

3. Results

For the diffusion time used here, experimental *RMSDs* measured (Fig.1, 2) are in the same order as those calculated for viscous cytoplasm. However, cell water diffusion propagator is not gaussian, probably because water diffuses in a less viscous, but structured media whose size is in the order of the length scale of brain cells diameter (glial cell, 2.5-9 µm; neuron, ~5-20 µm [16]; dendritic tree arborescence, 13 µm diameter). Considering the imbrication and ramifications of cellular spaces, water mainly probes dense intracellular and extracellular matrix [17], and is able to diffuse towards the actin cytoskeleton [17] lattice mesh (0.1-1 µm), the tubulin/tau cytoskeleton network and to some packed axons (~0.5-2.5 µm diameter). A mean effect of the diffusion anisotropy at high *b* could decrease independently the *ADC* [17]. We made *q*-space signal simulations with variation of the anomalous exponent, kurtosis and of the diffusion coefficient. We found in healthy tissue the GM more anomalous than the WM. Simulated data compared to observed brain signals are presented in Fig.1. A limitation of qSI is that if the *P(RMSD=0)* is an hypothese-free parameter, the deducted *RMSD* is under gaussian phase approximation. Decreasing *D* raises the *P(RMSD=0)* but the propagator still remains gaussian (S3). Decreasing α (S2) or increasing kurtosis (S1) raise the peakedness of the initially gaussian propagator shape distribution and raise as well the *P(RMSD=0)*. This increase of the *P(RMSD=0)* characterizes the differences between both healthy GM versus healthy WM and healthy versus ischemic tissue. Thus, to explain changes in healthy/ischemic tissue or in GM/WM contrast difference, we may invoke both a modulation of the water diffusion coefficient itself (linked in our interpretation to the water viscosity) and of a parameter representing a structural feature of the media, both acting on the *RMSD* determination. In ischemic GM, the rise in viscosity probably result from the associated loss of structural features because water diffusion becomes closer to gaussian when *DCC* and *ADCk* decrease (Fig. 2).

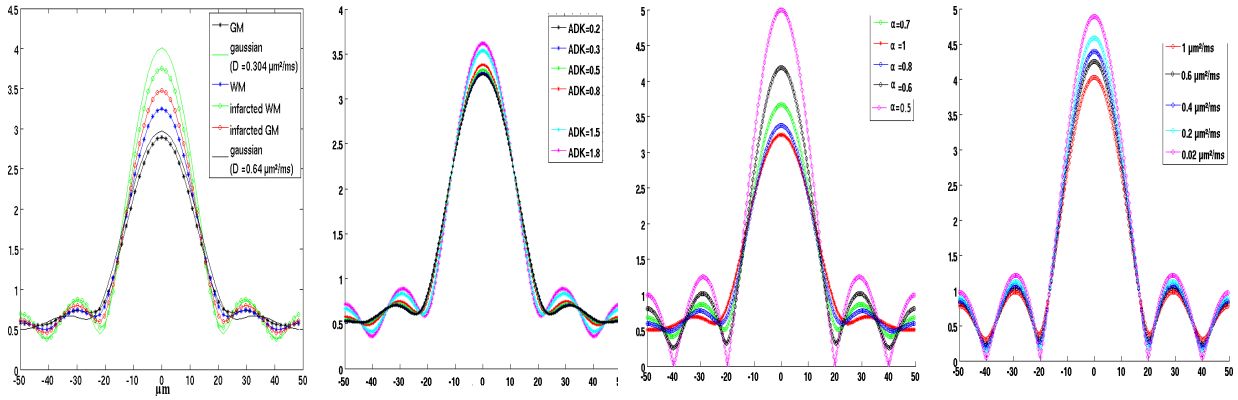

	Experimental			Simulation (S1)			Simulation (S2)			Simulation (S3)		
Signal	***RMSD* (µm)**	***P(RMSD=0)***		***ADK***	***RMSD* (µm)**	***P(RMSD=0)***	***α***	***RMSD* (µm)**	***P(RMSD=0)***	***D* (µm²/ms)**	***RMSD* (µm)**	***P(RMSD=0)***
WM	**11.95315**	3.25043		***ADK*=0.5**	**11.95310**	3.32430	***α*=1**	**12.28515**	3.244405	**1**	**10.62500**	4.02410
Ischemic WM	**10.95703**	3.75542		***ADK*=0.8**	**11.62110**	3.37940	***α*=0.8**	**11.621093**	3.377006	**0.6**	**10.29296**	4.24850
GM	**12.61718**	2.89380		***ADK*=1.5**	**11.28910**	3.53520	***α*=0.7**	**10.95703**	3.66812462	**0.4**	**10.29296**	4.39420
Ischemic GM	**11.28906**	3.47904		***ADK*=1.8**	**10.95700**	3.61630	***α*=0.6**	**10.29296**	4.1858259	**0.2**	**10.29296**	4.58610

Fig. 1 Diffusion propagators (p_s) resulting from averaging of localized magnetization DDI signal for WM, ischemic WM, GM, ischemic GM. *P(RMSD=0)* is the peak maximum intensity. *RMSD* is defined as the lateral gaussian width (0.425x*FWHM*). Simulations with increased kurtosis and *α* are realized with *D*=0.7 µm²/ms. *α*=0.6 for increased *D* (S3).

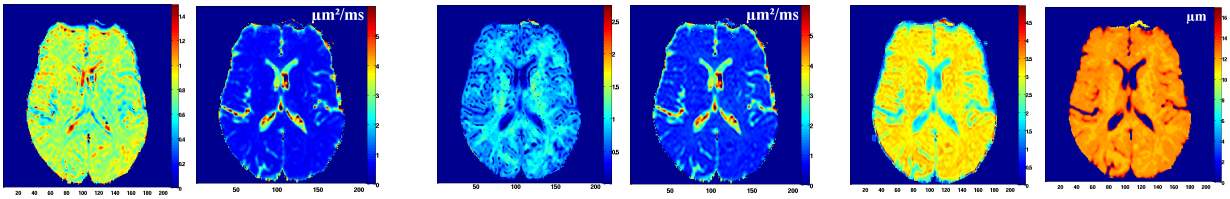

α ***DDC*** ***ADK*** ***ADCk*** ***P(RMSD=0)*** ***RMSD***

MEDI	***ADC*** ± SD(***ADC***) µm²/ms	***RMSD***		DKI	***ADCk*** ± SD(***ADCk***) µm²/ms	**RMSD**	***ADK*** ± SD(***ADK***)
WM	0.58179± (3.060242x10^{-3})	**9.73210**		**WM**	0.91204± (7.28192x10^{-2})	**12.18520**	0.82877±0.0029386
Ischemic WM	0.14488± (1.6255x10^{-4})	**4.85660**		**Ischemic WM**	0.24202± (1.21010x10^{-3})	**6.27700**	0.76687± 0.0034765
GM	0.73790± (5.91233x10^{-5})	**10.96030**		**GM**	1.28210± (8.76839x10^{-2})	**14.44730**	0.72296± 0.0028751
Ischemic GM	0.48258± (5.91235x10^{-3})	**8.86360**		**Ischemic GM**	0.71240±(6.00953x10^{-4})	**10.79630**	0.98034± 0.003140

BEDI	F_{fast}± SD(F_{fast})	ADC_{fast}± SD(ADC_{fast}) µm²/ms	***RMSD***	F_{slow}± SD(F_{slow})	ADC_{slow} ± SD(ADC_{slow}) µm²/ms	***RMSD* (µm)**
WM	0.64706 ± (7.34166x10^{-4})	1.54561± (1.79224x10^{-1})	**15.86260**	0.35293±(7.34165x10^{-4})	0.24997± (8.2085x10^{-3})	**6.37920**
Ischemic WM	0.716373±0.0015449	0.97553± (2.61919x10^{-2})	**12.60220**	0.28372±(2.95026x10^{-4})	0.075699±(7.1855x10^{-4})	**3.51050**
GM	0.58308±0.0014755	2.90698± (4.42770x 10^{-2})	**21.75430**	0.41691±0.0014755	0.39054± (4.75185x10^{-4})	**7.97370**
Ischemic GM	0.45766 ±0.0043817	2.34798± (1.14529x10^{-1})	**19.55110**	0.54233±0.0043817	0.28790±(1.29983x10^{-3})	**6.84610**

DKI	***ADK*** ± SD(ADK)	***ADCk*** ± SD(***ADCk***) µm²/ms	***RMSD***	ADI	***DDC***± SD(***DDC***) µm²/ms	***RMSD***	α ± SD(α)	d_*
WM	0.82877±0.0029386	0.91204 ±(7.28192x10^{-2})	**12.18520**	**WM**	0.65056±(2.5639 x10^{-3})	**10.29130**	0.83293± 0.0026382	2.40114
Ischemic WM	0.76687±0.0034765	0.24202 ±(1.21010x10^{-3})	**6.27700**	**Ischemic WM**	0.13538± (1.47100x10^{-4})	**4.69460**	0.32889±0.001187	6.08106
GM	0.72296±0.0028751	1.28210±(8.76839x10^{-2})	**14.44730**	**GM**	0.95598±(1.78523x10^{-3})	**12.47520**	0.78473± 0.002778	2.54864
Ischemic GM	0.98034±0.003140	0.71240±(6.00953x10^{-4})	**10.76930**	**Ischemic GM**	0.518328± (1.03380x10^{-3})	**9.18600**	0.81224± 0.0012935	2.4623264

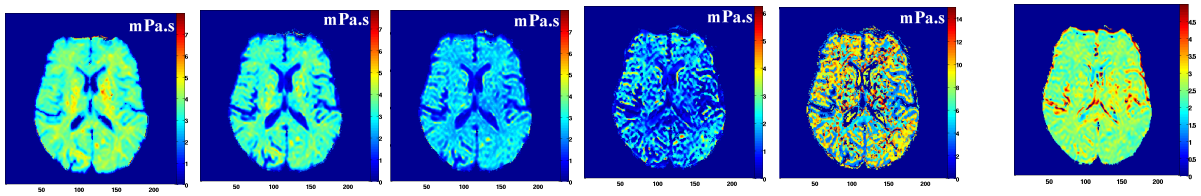

η(ADC) ***η(DCC)*** ***η(ADCk)*** ***η(D_{fast})*** ***η(D_{slow})*** ***d_w***

Fig. 2 On top, images showing the contrast between GM/WM results from pixel-by-pixels fitting of DDI, taken from the a slightly infarcted area. Table : spatial mean of fit parameters images and calculated RMSD for different DDI modelling (mean ± standard deviation). On bottom, d_w and viscosity maps calculated with Stokes-Einstein. One can note that, contrary to *η(ADC)* and to a little extent to *η(DCC)* maps, *η(ADCk)* do not present any WM/GM contrast.

4. Discussion

Recently, it has been hypothesized that cytoskeleton is the biological structure causing non-monoexponential water diffusion decay [17]. Cytoskeleton crowded network has been shown to be responsible of the anomalous diffusion properties of probes [4,6,7,8]. In a subcellular point of view, GM is mainly constituted of actin and associated proteins, and WM, of tubulin and neurofilaments (with a few perimembranar actin). Microtubules are empty cylinders, 50-100 μm length, 25 nm diameter. Tubulin polymerization is GTP-dependant and ATP depletion by ischemia induces a destructuration of the microtubules with the loss of the axonal transport and the liberation of free tubulin [18], that could explain the *ADC* decrease (high water viscosity) in infarcted WM. Various chemotherapy drugs acting on microtubules have been shown to decrease WM *ADC* [19], as microtubule polymerisation inhibitors like Taxol, that causes an *ADC* decrease when injected in a tumor site [20] and vinblastine (preserving neurofilaments) that leads to *ADC* decrease in both perpendicular and parallel directions to the axon, together with conserved diffusion anisotropy [22]. If microtubules dissociation with nocodazole do not change the *ADC* in *Xenopus* oocytes [21], in nerves, it has been shown that the microtubule depolymerizer methylmercury rises the diffusion of water in axonal longitudinal direction [23]. Imidinodipropionitrile, causing the displacement of neurofilaments to the axon periphery, with microtubule moving to the center of the axon, induces in the spinal chord F_{slow} increase and D_{slow} decrease [24], the latter being responsible of the high *b*-value WM vs GM contrast [25] corresponding to an *ADC* decrease in WM. As diffusion probes a length scale of the cellular size order, water would be sensitive to the viscosity of the space traversed during the random walk, additionally affected by collision (and perhaps, binding) of water with local intra/extracellular microstructures [1,3], the latter causing a departure from gaussian diffusion. Disrupting cytoskeleton by ischemia (and with some chemicals) causes an α decrease representing the increase of the fractal dimension (higher order structure scale that water meets during diffusion), characterized by a peakedness of the gaussian distribution, together with a decreased diffusion coefficient that could be representative of increased viscosity in the stroke zone by a sol to a viscous gel transition. In conclusion, the use of the complete propagator informations, instead of ADC [1] would give valuable information about subcellular structures that have a functional role in cells, bridging the gap between the cell ultrastructure and energetic metabolism, both affecting the water diffusion signal. However, for qSI-based images extraction, some propagator informations are lost.

5. References

[1] D.S Grebenkov, Concepts in Magnetic Resonance Part A 36A (2010) pp. 24-25.
[2] A.S. Verkman, TRENDS in Biochemical Sciences 27(1) (2002) pp. 27-33.
[3] D.S. Novikov, V.G. Kiselev, NMR in Biomedecine, 23 (2010) pp. 682-697.
[4] M. Weiss, M. Elsner, F. Kartberg, T. Nilsson, Biophysical Journal 87(5) (2004) pp. 3518–3524.
[5] M. Köpf, C. Corinth, O. Haferkamp, T.F. Nonnenmachert, Biophysical Journal 70 (1996) pp. 2950-2958.
[6] D.S. Banks, C. Fradin, Biophysical Journal 89(5) (2005) pp. 2960–297.
[7] M. Tolic-Nørrelykke, E-L. Munteanu, G. Thon, Physical Reviews Letters 93(7) (2004) pp. 078102-1 – 078102-4.
[8] Y. Wong, M. L. Gardel, D.R. Reichman, Physical Reviews Letters 92(17) (2004) pp. 178101-1– 178101-4.
[9] A. Schwarcz, P. Bogner, P. Meric, J-L Correze, Magnetic Resonance in Medicine 51(2) (2004) pp. 278-285.
[10] L.Korson, W. Drost-Hansen, F.J. Millero, The Journal of Physical Chemistry 73(1) pp. 34-39.
[11] C.A. Clark, D. Le Bihan, Magnetic Resonance in Medicine 44 (2000) pp. 852– 859.
[12] K. Luby-Phelps, International Reviews of Cytology 192 (2000) pp. 189-221.
[13] M. G. Hall, T.R .Barrick, Magnetic. Resonance in Medecine 59 (2008) pp. 447-455.
[14] K. Bennett, K. Schmainda, R. Bennett , D. Rowe, Magnetic Resonance in Medecine 50 (2003) pp. 727-734.
[15] J.H Jensen, JA Helpern, A Ramani, H. Lu, Magnetic Resonance in Medecine 53 (2005) pp.1432-1440.
[16] G. Rajkowska, L D. Selemon, P. S. Goldman-Rakic, Archives of General Psychiatry 55 (1998) pp. 215-224.
[17] D. Le Bihan, Physics in Medicine and Biology 52(7) (2007) pp. R57-R90.
[18] M.A. Petty, J.G. Wettstein, Brain Research Review 31(1) (1999) pp. 58-64.
[19] C.S. Tam, J. Galanos, J.F. Seymour, A.G. Pitman, American Journal of Hematology 77 (2004) pp. 72–76.
[20] Y. Mardor, Y. Roth, Z. Lidar, V. Jonas, R.Pfeffer, SE Maier, Cancer Research 61 (2001) pp. 4971-4973.
[21] FJ.V. Sehy, L. Zhao, J. Xu , H.J. Rayala, Magnetic Resonance in Medecine 52(2) (2004) pp. 239-247.
[22] C. Beaulieu, P.S. Allen, Magnetic Resonance in Medecine 31 (1994) pp. 394-400.
[23] Y. Kinoshita, A.Ohnishii, K.Kohshi A.Yokota, Environmental Research Section A 80 (1999) pp. 348-354.
[24] T.M. Shepherd , P.E. Thelval, E.D. Wirth, Proceeding of the ISMRM 2011 9 (2001) pp. 1624.
[25] S.E. Maier, R.V. Mulkern, Magnetic Resonance Imaging 26 (2008) pp. 897-904.

Acknowledgments

V. Kiselev, D. Le Bihan, J.H. Jensen, J.M. Franconi, P. Voisin, E. Thiaudière, R. Mulkern, Y. Monneau, B. Dhital.